

STELLAR ATMOSPHERES, ATMOSPHERIC EXTENSION AND FUNDAMENTAL PARAMETERS:
WEIGHING STARS USING THE STELLAR MASS INDEXHILDING R. NEILSON¹, FABIEN BARON², RYAN NORRIS², BRIAN KLOPPENBORG², AND JOHN B. LESTER^{1,3}*Draft version June 28, 2021*

ABSTRACT

One of the great challenges in understanding stars is measuring their masses. The best methods for measuring stellar masses include binary interaction, asteroseismology and stellar evolution models, but these methods are not ideal for red giant and supergiant stars. In this work, we propose a novel method for inferring stellar masses of evolved red giant and supergiant stars using interferometric and spectrophotometric observations combined with spherical model stellar atmospheres to measure what we call the stellar mass index, defined as the ratio between the stellar radius and mass. The method is based on the correlation between different measurements of angular diameter, used as a proxy for atmospheric extension, and fundamental stellar parameters. For a given star, spectrophotometry measures the Rosseland angular diameter while interferometric observations generally probe a larger limb-darkened angular diameter. The ratio of these two angular diameters is proportional to the relative extension of the stellar atmosphere, which is strongly correlated to the star's effective temperature, radius and mass. We show that these correlations are strong and can lead to precise measurements of stellar masses.

Subject headings: stars: atmospheres — stars: fundamental parameters — stars: late-type — supergiants — techniques: interferometric

1. INTRODUCTION

Red giant and supergiant stars represent a crucial stage of stellar evolution where stars fuse elements heavier than hydrogen as they approach the end of their lives before they explode as core-collapse supernovae, driving the next generation of star formation, or shed their envelopes on the evolutionary path to becoming white dwarfs. These stars have the largest radii of all stars and therefore, are ideal targets for optical interferometric observations (*e.g.* Kloppenborg & van Belle 2015).

Interferometric observations of red supergiant stars have provided insights into center-to-limb intensity variation (CLIV), also known as limb darkening, convection, deviations from spherical symmetry, and circumstellar material (Haubois et al. 2009; Ohnaka et al. 2011, and others). While these observations are powerful and insightful, there exist many challenges for interpreting these measurements and determining fundamental stellar parameters, such as mass. The measurement of stellar mass is especially problematic because there are only a few viable methods, some of which are sensitive to other processes, such as internal mixing and mass loss.

There are two primary tools for inferring stellar masses of single giant and supergiant stars: stellar spectroscopy and stellar evolution modelling. The latter method requires knowledge of many other fundamental parameters such as effective temperature and luminosity. However, red giant and supergiant stars of different masses converge to similar effective temperatures near

the Hayashi line on the Hertzsprung-Russell diagram (Kippenhahn et al. 2012; Ekström et al. 2012). For example, Dolan et al. (2016) determined the mass of Betelgeuse by fitting stellar evolution models to measurements of its radius, effective temperature and mass-loss rate and found a mass of about $20 M_{\odot}$. This value, however, depends on the treatment of mass loss, core convection, and internal mixing in the stellar evolution models, which in turn limits the robustness of the determination.

Similarly, stellar spectra are ideal for measuring effective temperatures, surface gravities and compositions (*e.g.* Gray 2005). For example, Lobel & Dupree (2001) measured $\log_{10} g \approx -0.5$ for Betelgeuse. However, this value is also sensitive to turbulence and convective velocities (Gray & Pugh 2012), increasing the uncertainty of the final estimated mass.

Neilson & Lester (2011) and Lester et al. (2013) showed it is possible to infer a star's mass from the extension of the atmosphere by using measurements of the star's CLIV and stellar atmospheric models. Neilson et al. (2011) measured a mass for Betelgeuse to be about $12 - 16 M_{\odot}$, much smaller than found using stellar evolution models. While that method depended on limb-darkening laws (*e.g.* Claret 2000; Claret & Bloemen 2011; Neilson & Lester 2013a,b), it suggested the possibility of applying measurements of atmospheric extension for inferring stellar masses.

Optical interferometry measures both the angular diameter and stellar CLIV (Davis et al. 2000). Wittkowski et al. (2004) attempted to fit stellar atmosphere model intensity profiles directly to interferometric and spectrophotometric observations of a red giant star. Although they were unable to distinguish between different stellar atmosphere models, they did measure precisely the limb-darkened and Rosseland angular diameters. Similar results were obtained for other red giant stars (Wittkowski et al. 2006b,a). A key is-

Electronic address: neilson@astro.utoronto.ca

¹ Department of Astronomy & Astrophysics, University of Toronto, 50 St. George Street, Toronto, ON, M5S 3H4, Canada² Center for High Angular Resolution Astronomy, Department of Physics and Astronomy, Georgia State University, P. O. Box 5060, Atlanta, GA 30302-5060, USA;³ Department of Chemical & Physical Sciences, University of Toronto Mississauga, Mississauga, ON L5L 1C6, Canada

sue was that these studies had to assume stellar parameters for the atmosphere models. But using a grid of model stellar atmospheres computed as described in Lester & Neilson (2008), Neilson & Lester (2008) were able to fit both spectrophotometric and interferometric observations used by Wittkowski et al. (2004, 2006b,a) without assuming any stellar parameters. The resulting models reliably reproduced the measured Rosseland and limb-darkened angular diameters.

However, for both analyses stellar masses were inferred from stellar evolution tracks; fitting model stellar atmospheres did not constrain the masses of the stars. The combination of interferometric and spectrophotometric observations alone are currently insufficient for measuring stellar masses. There are not, as of yet, methods to measure masses directly from fitting model stellar atmospheres to observations with any significant precision.

The purpose of the present work is to develop a new method for inferring stellar fundamental parameters from interferometric and spectrophotometric observations using spherical model stellar atmospheres. This approach is based on the previous work of Neilson & Lester (2012) who found that coefficients from a specific limb-darkening law are correlated with the atmospheric extension. In this work, we completely abandon the concept of arbitrary limb-darkening laws with adjustable coefficients, which in practice are poorly constrained by measurements. In the next section we develop proxies for atmospheric extension based on spectro-interferometric measurements, tying them to fundamental parameters, especially stellar masses. In Section 3, we outline the spherical model stellar atmospheres used in this work and present the best-fit correlations in Section 4 along with a comparison to previous measurements. We summarize our work in Section 5.

2. ATMOSPHERIC EXTENSION AND THE STELLAR MASS INDEX

Neilson & Lester (2012) showed that for spherically symmetric model stellar atmospheres the coefficients used to fit the CLIV depend on the amount of atmospheric extension, denoted by the ratio of the stellar radius to mass, R/M in solar units. The stellar radius is defined as the point in the star where the Rosseland optical depth is 2/3 (Mihalas 1978). Here we define this ratio as the stellar mass index (SMI),

$$\text{SMI} \equiv \frac{R_{\text{Ross}}}{M} (R_{\odot}/M_{\odot}). \quad (1)$$

The SMI is analogous to a person's body mass index, the ratio of a person's height and weight. These results suggest that a measurement of atmospheric extension can provide information about fundamental stellar parameters, potentially without requiring knowledge of distances.

Following the approach of Baschek et al. (1991) and Bessell et al. (1991), Neilson & Lester (2012) represented the relative extension of a stellar atmosphere as

$$\frac{\Delta R}{R_{\text{Ross}}} \propto \frac{H_P}{R_{\text{Ross}}} \equiv \frac{kT_{\text{eff}}/\mu m_H g}{R_{\text{Ross}}}, \quad (2)$$

where H_P is the pressure scale height and where $\Delta R \equiv R_{\text{LD}} - R_{\text{Ross}}$ is the difference between R_{LD} , the radius at the top of the atmosphere, and R_{Ross} , the Rosseland radius. The variables μm_H represents the mean

atomic mass in the atmosphere, independent of mass or radius for a given atmospheric composition. Using $g \propto M_{\star}/R_{\text{Ross}}^2$ gives

$$\frac{\Delta R}{R_{\text{Ross}}} \propto T_{\text{eff}} \left(\frac{R_{\text{Ross}}}{M_{\star}} \right) = T_{\text{eff}} \times \text{SMI}. \quad (3)$$

This suggests that the stellar mass is defined, along with the gravity, at the Rosseland radius and not at the limb-darkening radius. But, because the density in the photosphere is orders of magnitude smaller than in the stellar envelope and core, the difference in stellar mass at the Rosseland and at the limb-darkening radius is negligible.

The theoretical definition of R_{LD} involves the minimum optical depth of the photosphere and hydrostatic equilibrium: the boundary condition at the top of the photosphere implies that the pressure and density go to zero. Consequently the precise value of the radius at the top of the photosphere is model dependent: it depends on the hydrostatic equilibrium in the model, i.e., on the gravity of the stellar atmosphere. In practice, boundary conditions are imposed by positing an actual minimum optical depth in model atmosphere codes (see e.g., section 4 for the adopted value in ATLAS/SATLAS). Different reasonable choices for this minimum optical depth lead to slightly different values R_{LD} ; however this spread in values remains insignificant for our purpose, being at least two orders of magnitude below expected ΔR .

The $\Delta R/R_{\text{Ross}}$ defined above can be measured empirically employing a combination of spectrophotometry and interferometry (e.g. Wittkowski et al. 2004; Neilson & Lester 2008). Observing the unresolved star's spectral energy distribution, it is possible to determine the bolometric flux, F_{bol} , which depends on the star's angular diameter and effective temperature

$$F_{\text{bol}} = 4\pi\theta_{\text{Ross}}^2\sigma T_{\text{eff}}^4, \quad (4)$$

where θ_{Ross} is the angular diameter at the Rosseland radius. Interferometry measures spatial frequencies, from which one can infer the whole CLIV, hence a size scaling factor for any given limb-darkening profile. When combined with model stellar atmospheres, it is possible to determine the angular diameter where the intensity approaches zero and the optical depth approaches zero ($\theta_{\tau \rightarrow 0}$) which is designated θ_{LD} (e.g. Lester et al. 2013). As Wittkowski et al. (2004) have shown, θ_{LD} is different from θ_{Ross} . The two angular diameters are not independent variables but they can be independently measured using different methods.

Rewriting Equation 3 as a function of angular diameters rather than linear radii leads to the expression:

$$M_{\star} \propto T_{\text{eff}} \frac{\theta_{\text{Ross}}^2 d/2}{\theta_{\text{LD}} - \theta_{\text{Ross}}}, \quad (5)$$

where d is the distance to the star and we replace $R_{\text{Ross}} = d\theta_{\text{Ross}}/2$. This indicates the SMI can be determined from angular diameters derived from a combination of spectrophotometric and interferometric observations. Testing the correlation between the relative atmospheric extension $\Delta R/R_{\text{Ross}}$, or its observed proxy $(\theta_{\text{LD}} - \theta_{\text{Ross}})/\theta_{\text{Ross}}$, and $T_{\text{eff}}(R_{\text{Ross}}/M_{\star})$ is the primary goal of this article.

To summarize this method, one can measure stellar masses using this relation plus interferometric and spectrophotometric observations in the following steps:

- i) from spectrophotometric observations measure the combination of the effective temperature and Rosseland angular diameter;
- ii) use a grid of model stellar atmospheres to fit interferometric observations to measure the limb-darkened angular diameter;
- iii) take the combination of the Rosseland and limb-darkened angular diameters to measure $R_{\text{Ross}}/M_{\star}$;
- iv) and measure the radius of the star using an independent distance measurement plus the Rosseland angular diameter and then measure the stellar mass from the value of $R_{\text{Ross}}/M_{\star}$.

There are other paths to measure the stellar mass using the SMI correlation. For instance, one can simultaneously fit the Rosseland angular diameter and effective temperature from spectrophotometry, the limb-darkened angular diameter from interferometric observations and apply our correlation as a constraint for the measurements to build a statistical fit of the fundamental stellar properties using grids of model stellar atmospheres. Alternatively, one can assume an estimate for stellar properties, compute a single model stellar atmosphere to fit the interferometric observations and then measure a new value for mass using our correlation. From that measurement, we can compute a new model stellar atmosphere and repeat the process until the predicted values of mass converge.

We note that our method takes advantage of the physics of model stellar atmospheres to refine measurements of stellar parameters in an already model-dependent analysis. All angular diameter measurements from interferometric observations to this point have assumed a model for stellar limb darkening, be it parametric, uniform disk, or a more-realistic model stellar atmosphere.

In terms of the intensity profile and fitting interferometric observations, we should ask what is the radius we measure. Because interferometric observations are fit assuming some model of the intensity profile then the corresponding best-fit angular diameter is a function of that intensity profile in the limit of $\mu \rightarrow 0$. When one assumes a uniform-disk intensity profile, one measures an angular diameter that is scaled by the flux. When one assumes a plane-parallel model stellar atmosphere CLIV, then it is possible to measure a value of the Rosseland angular diameter, but only because plane-parallel atmospheres have no information of radius by definition. The CLIV for spherically symmetric model atmospheres is far more complex and contains information of radius. The top of the photosphere, R_{LD} , corresponds to the point where $\mu = 0$, hence the measured angular diameter will correspond to the R_{LD} . But, because the interferometric visibilities are the Hankel transform of the CLIV then the observations will be strongly weighted by the point where the CLIV drops off most rapidly. That layer is approximately the Rosseland radius.

Because of these issues, any attempts to measure the limb-darkened angular diameter requires interferometric visibilities that probe at least the second lobe of the visibility curve where differences in limb darkening at the edge of the stellar disk offer the greatest weight in

the Hankel transform. This implies that our proposed method is most useful for interferometric observations that reach baselines beyond the first minimum.

Furthermore, one might expect that fitting interferometric observations using model stellar atmospheres will allow one to uniquely measure the stellar mass. Neilson & Lester (2008) found that the best-fit limb-darkening angular diameter from interferometric observations do not yield unique measurements of stellar properties. Lester et al. (2013) presented a study of CLIV and spectra as a function of stellar mass. If one knows precisely the stellar radius and effective temperature, then the stellar mass can be, at best, measured to a precision of a factor of a few. Therefore, the combination of interferometric and spectrophotometric (or spectroscopic) observations is insufficient to measure stellar masses with any meaningful precision; our SMI correlation is crucial to improve those measurements.

3. MODEL STELLAR ATMOSPHERES

To test for the correlations suggested, we use a grid of model stellar atmospheres computed using the SATLAS code (Lester & Neilson 2008; Neilson & Lester 2013a). These models are hydrostatic, spherically symmetric and use opacity distribution functions constructed from approximately two million atomic/ionic lines and eight million molecular lines extending to temperatures down to 2000 K (Castelli & Kurucz 2010; Kurucz 2011). Convection is treated using the standard mixing length theory (Vitense 1953; Böhm-Vitense 1958). This code is built upon the earlier ATLAS codes developed by Kurucz (1970). The SATLAS code computes intensities and fluxes as a function of wavelength assuming local thermodynamic equilibrium that can be applied to spectroscopic, photometric and interferometric observations.

One caveat regarding the code is the omission of the extended molecular layers or MOLsphere (Tsuji 2000) of red supergiant stars. However, it should be noted that for many wavelengths the MOLsphere does not affect either the calculations or observations. For example, observations of Betelgeuse in the H -band (Haubois et al. 2009), a spectral band where the outer molecular layers would be expected to make a larger contribution, did not detect the MOLsphere. Furthermore, as of yet no model stellar atmosphere codes properly model the MOLsphere and interferometric observations of stars with MOLspheres can be interpreted in terms of multicomponent models such as a model stellar atmosphere CLIV plus an analytic MOLsphere component (Montargès et al. 2014). That type of model limits bias in the measurement of θ_{LD} . Similar biases, such as star spots and rotation, can also impact our method, but it is up to the observer to carefully interpret interferometric observations.

The grid of spherical models used here spans $T_{\text{eff}} = 3000$ to 8000 K in steps of 100 K, $\log g = -1$ to $+3$ in steps of 0.25 dex and masses $M_{\star} = 0.5, 1, 2.5, 5, 7.5, 10, 12.5, 15, 17.5, 20 M_{\odot}$, although the parameter space has some gaps where models failed to converge. This grid of models was used by Neilson & Lester (2013a) to compute limb-darkening coefficients, angular diameter corrections for interferometric observations and gravity-darkening coefficients. Figure 1 plots the model parameter space on a spectroscopic Hertzsprung-Russell diagram (Langer & Kudritzki 2014)

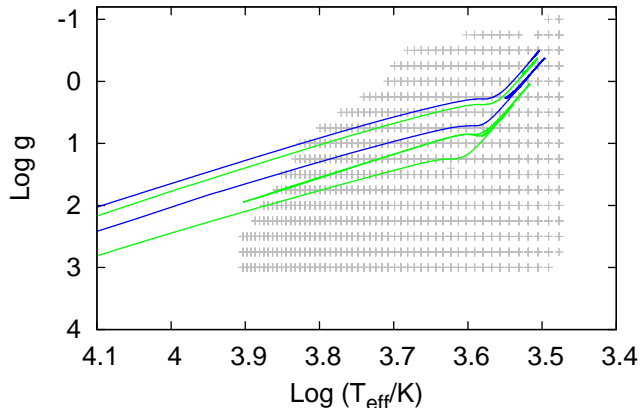


FIG. 1.— Spectroscopic HR diagram denoting the parameter space in T_{eff} and $\log g$ of the stellar atmosphere models considered in this work. The plus symbols represent the T_{eff} and $\log g$ of the individual model atmospheres used in this study. The solid lines are post main-sequence evolutionary tracks for stars with masses 8 to 20 M_{\odot} from Neilson et al. (2012a,b).

along with a sample of stellar evolution tracks for masses from 8 to 20 M_{\odot} (Neilson et al. 2012a,b).

For each spherical model stellar atmosphere in the grid, the intensity is computed as a function of μ , which is defined as the cosine of the angle formed between the normal vector at a point on the stellar surface and the direction toward the distant observer. The intensity was computed for 1,000 equally spaced points in μ -space, making these the most detailed intensity profiles published (Neilson & Lester 2013a,b).

4. RESULTS

For each spherical model stellar atmosphere in the grid we compute the surface radius $R_{\tau \rightarrow 0}$, which we consider to be the limb-darkened radius. In addition to this limb-darkening radius and the Rosseland radius $R_{\tau=2/3}$, we also have the uniform-disk radii for interferometric observations from Neilson & Lester (2013a), which is defined as the stellar radius necessary to fit interferometric visibilities assuming the CLIV is constant across the stellar disk. It should be noted that the calculations by Neilson & Lester (2013a) predicted the relative uniform-disk correction, i.e., $R_{\text{UD}}/R_{\text{LD}}$ or $R_{\text{UD}}/R_{\text{Ross}}$ and not the absolute uniform-disk values.

This correlation is computed for SATLAS stellar atmosphere models and is based on the parameters describing each model. In particular, SATLAS defines the limb-darkened radius where $\tau_{\text{Ross}} \rightarrow 0$. Slightly different assumptions and implementations used in other codes, such as PHOENIX (Hauschildt et al. 1999) and MARCS (Gustafsson et al. 2008), might yield slightly different results.

The value of the limb-darkened radius and θ_{LD} depends on the definition adopted for the star’s surface as the limit where $\tau_{\text{Ross}} \rightarrow 0$. For example, the ATLAS/SATLAS codes retain the original Kurucz (1970) location of the top of the atmosphere at $\tau_{\text{Ross}} = 1.334 \times 10^{-6}$ ($\log_{10} \tau_{\text{Ross}} = -5.875$). This choice of the surface τ_{Ross} , however, has essentially no effect on the physical radius because the gas density is so low. As an example, for a typical red giant model atmosphere with $L_{\star} = 500 L_{\odot}$, $M_{\star} = 1 M_{\odot}$ and $R_{\star} = 50 R_{\odot}$, redefining the physical radius to the location where the Rosseland

optical depth is $100\times$ larger than the value adopted here reduces the radius by less than $0.1\times$ our uncertainty of $(\theta_{\text{LD}} - \theta_{\text{Ross}})$, but has no effect on the fit to interferometric data. The definition of θ_{LD} is a convention that depends on the CLIV. As long as the same definition is used by both stellar atmosphere models and by the model fit to interferometric data, θ_{LD} acts strictly as a spatial scaling parameter for the CLIV profile. Thus it possesses a unique, non-ambiguous nominal value. We note, however, that the θ_{LD} conventions will be equivalent to θ_{Ross} only in the limit where the atmospheric extension goes to zero. We conclude that our definition of the limb-darkened radius, although model dependent, is still a useful tool for interferometric observations, especially when the model intensity profiles are used to fit those observations.

4.1. Correlations

For the first test, we search for correlations between the atmospheric extension $(\theta_{\text{LD}} - \theta_{\text{Ross}})/\theta_{\text{Ross}}$ and a measure of $T_{\text{eff}} \times \text{SMI}$. In Figure 2, we plot the two measurements and confirm the existence of a linear correlation. Models with $T_{\text{eff}} \leq 3200$ K are shown in gray, but they are not used in fitting the correlations because at low temperature the model stellar atmospheres do not converge as well, implying a significant flux error that will bias any fit. The best-fit relation is

$$\left(\frac{T_{\text{eff}}}{T_{\text{eff},\odot}}\right) \left(\frac{R_{\text{Ross}}}{M_{\star}}\right) = (565.99 \pm 0.96) \frac{\theta_{\text{LD}} - \theta_{\text{Ross}}}{\theta_{\text{Ross}}}. \quad (6)$$

This is a strong correlation, confirming our expectations from the previous sections. However, we note that the data points for $(\frac{T_{\text{eff}}}{T_{\text{eff},\odot}})(\frac{R_{\text{Ross}}}{M_{\star}}) > 120 \frac{R_{\odot}}{M_{\odot}}$ drift above the best-fit straight line, which is dominated by the large number of points $\leq 120 \frac{R_{\odot}}{M_{\odot}}$. This drift could be due to a change in the dominant opacity for the most extended models, which are also the stars with the lowest effective temperatures. This deviation deserves further investigation, but for the purposes of this work we consider only a linear fit.

Because of the deviation in the plots in the left panel of Figure 2, we also fit a slightly different correlation, $\Delta\theta/\theta_{\text{LD}}$, instead of normalizing with respect to θ_{Ross} . There is no obvious justification for this revised relation, but the correlation is stronger, particularly at large atmospheric extensions.

$$\left(\frac{T_{\text{eff}}}{T_{\text{eff},\odot}}\right) \left(\frac{R_{\text{Ross}}}{M_{\star}}\right) = (647.48 \pm 0.67) \frac{\theta_{\text{LD}} - \theta_{\text{Ross}}}{\theta_{\text{LD}}}. \quad (7)$$

A possible reason for this improvement is that at the largest extensions T_{eff} is greater, but the gravity is weaker. The radiation pressure is increased relative to the gas pressure, which makes it somewhat more numerically difficult to compute stable stellar atmospheres. This may result in an overestimation of the limb-darkened angular diameter, and thus in deviations of the parameter θ_{LD} at the largest extension, that the reformulated relation would then partially cancel out.

The second test is to measure the uniform-disk angular diameters from interferometric observations (*e.g.* Davis et al. 2000; van Belle et al. 2009) and lunar occultation observations (*e.g.* Richichi et al. 2014) and other

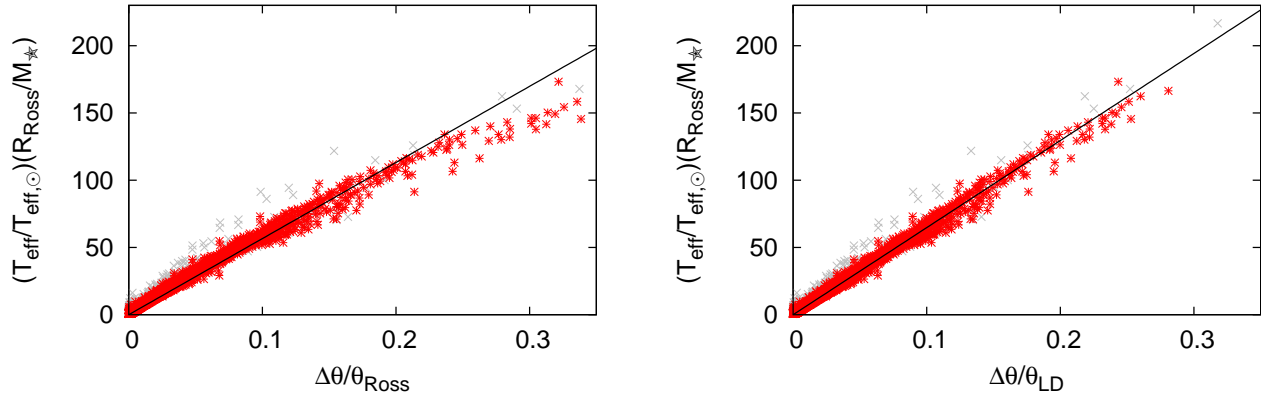


FIG. 2.— The correlation between the product of $T_{\text{eff}} \times \text{SMI}$ and the two proxies for the atmospheric extension. (Left) $(\theta_{\text{LD}} - \theta_{\text{Ross}})/\theta_{\text{Ross}}$. There is a correlation between the variables suggesting the potential for measuring fundamental stellar parameters from measurements of angular diameters, however, for large values of $(\theta_{\text{LD}} - \theta_{\text{Ross}})/\theta_{\text{Ross}}$ the models seem to follow a non-linear trend. (Right) An even stronger correlation is seen for the product of $T_{\text{eff}} \times \text{SMI}$ and $(\theta_{\text{LD}} - \theta_{\text{Ross}})/\theta_{\text{LD}}$.

methods. This is important because the more distant a star, the harder it is to resolve its second interferometric lobe. But one may still be able to measure the uniform-disk angular diameter in different wavelengths, and these have been tabulated over the years for various types of stars (*e.g.* van Belle et al. 2009; Boyajian et al. 2014; von Braun et al. 2014). We test various combinations of the uniform-disk, Rosseland and limb-darkened angular diameters for correlations with the atmospheric extension. While the Rosseland and limb-darkening angular diameters are independent of wavelength in the models, the uniform-disk radii are not. The limb-darkened angular diameters in the models are defined by the limit as $\tau_{\text{Ross}} \rightarrow 0$ and $\mu \rightarrow 0$.

In Figure 3 we plot the uniform-disk angular diameters computed from synthetic visibilities relative to the limb-darkened angular diameters (left) and Rosseland angular diameters (right) as functions of atmospheric extension. The correlations show greater scatter, but are still sufficiently strong to indicate that replacing θ_{Ross} by θ_{UD} in the atmospheric extension term defined in Equation 5 and shown in Figure 2 would still exhibit a significant correlation, even more so in *H*-band, indicating further exploration is warranted. Unfortunately, there appears to be no correlation between the SMI and the ratio $\theta_{\text{UD}}/\theta_{\text{Ross}}$, which indicates that for the worst possible case the correlations break down.

4.2. Testing Atmospheric Extension Correlations

As a consistency check, we use the results for χ Phe from Wittkowski et al. (2004), who measured an effective temperature $T_{\text{eff}} = 3550 \pm 50$ K and a Rosseland angular diameter $\theta_{\text{Ross}} = 8.0 \pm 0.4$ mas solely from spectrophotometric observations. Wittkowski et al. (2004) also derived a limb-darkened angular diameter of 8.65 ± 0.15 mas by fitting PHOENIX model stellar atmospheres to optical interferometric observations. These fits use an entirely different model atmosphere code than is used in our fits, but similar results can be found using SATLAS models (Neilson & Lester 2008). The values found by Wittkowski et al. (2004) give $\Delta\theta/\theta_{\text{Ross}} = \Delta R/R_{\text{Ross}} = 0.081 \pm 0.005$. Using this and the T_{eff} derived by Wittkowski et al. (2004) in our relation given in Equation 6 yields the $\text{SMI} = 74.5 \pm 5.7$ in solar units. Wittkowski et al. (2004) derived the radius to be

$85 \pm 10 R_{\odot}$. When we combine that radius with the SMI we get a stellar mass $M_{\star} = 1.14 \pm 0.22 M_{\odot}$. This is consistent with the value found by Wittkowski et al. (2004), but it uses a less demanding measurement of the Rosseland angular diameter and does not invoke stellar evolution models. If we use Equation 7 instead, we measure a mass $M_{\star} = 1.07 \pm 0.21 M_{\odot}$, which is slightly smaller, but consistent with our first estimate and the previous reports.

Assuming the best method is to measure θ_{Ross} from spectrophotometric observations, then we also have a robust measure of the effective temperature, which suggests using Equation 6 to find the SMI. To extract the stellar mass from the SMI we seem to require some independent measure of the radius, say by using the angular diameter and a measurement of the star's parallax. However, we do not necessarily require a measurement of the distance. If we have spectroscopic observations that allow for a fit of effective temperature and gravity, then we can combine the gravity and the SMI to extract both the Rosseland radius and the mass, and one also can use this method to find the distance to the star. To conclude, there are a number of potential methods to measure the stellar mass from our atmospheric extension, independent of observations of binary stars or asteroseismic relations (Huber et al. 2010; Kallinger et al. 2010; Stello et al. 2013).

5. SUMMARY

The goal of this work was to develop a new method for inferring stellar masses from measurements of atmospheric extension in stars. We use the previously published grid of SATLAS model stellar atmospheres (Neilson & Lester 2013a) and compute values of the Rosseland, limb-darkened and uniform-disk radii, where combinations of any two parameters are proxies for the atmospheric extension. We also show that another proxy for the atmospheric extension is $T_{\text{eff}} R_{\text{Ross}}/M_{\star}$, which leads us to define stellar mass index, $\text{SMI} \equiv R_{\text{Ross}}/M_{\star}$.

We develop a methodology for measuring stellar masses from the trio of model stellar atmospheres, interferometric observations and spectrophotometric observations. That method takes independent measurements of Rosseland and limb-darkened angular diameters and computes the stellar mass index, $R_{\text{Ross}}/M_{\star}$, from the combination

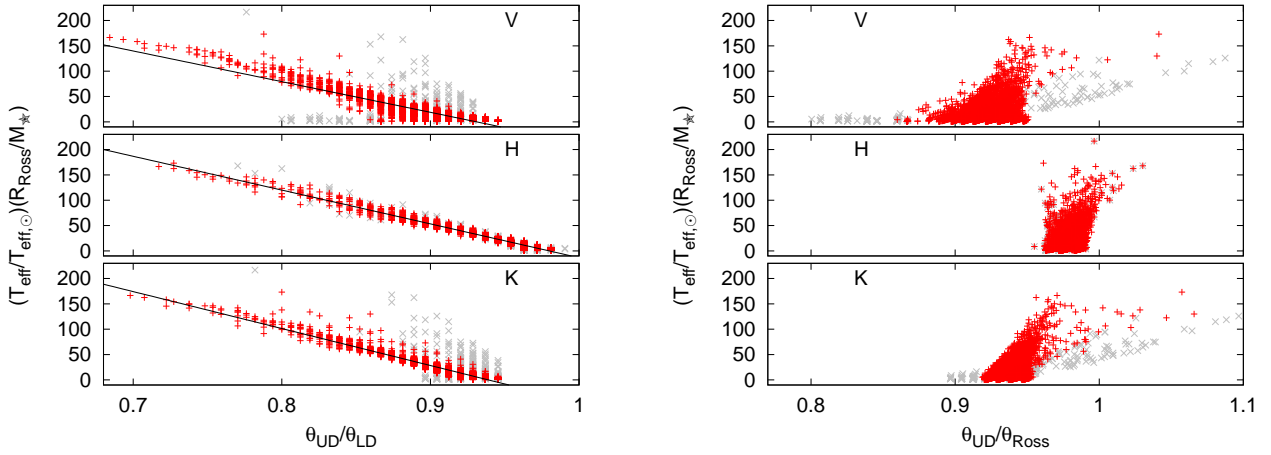


FIG. 3.— Correlation between the $T_{\text{eff}} R_{\text{Ross}}/M_{\star}$ and the proxies for the atmospheric extension, (left) $\theta_{\text{UD}}/\theta_{\text{LD}}$, (right) $\theta_{\text{UD}}/\theta_{\text{Ross}}$ for different wavebands: V, H, and K-band. Correlations are weaker when the uniform-disk angular diameters are considered, but trends are apparent for the ratio of $\theta_{\text{UD}}/\theta_{\text{LD}}$. There is no obvious correlation between $T_{\text{eff}} R_{\text{Ross}}/M_{\star}$ and the ratio $\theta_{\text{UD}}/\theta_{\text{Ross}}$ that suggests this is the limiting limb-darkening assumption for our method.

of the two diameters. With an independent measurement of the distance or the stellar gravity, then the mass can be measured without invoking stellar evolution tracks.

We then test these different proxies for correlations and find that the combination of Rosseland and limb-darkened radii are strongly correlated with the atmospheric extension, which provides a powerful method for inferring stellar parameters from interferometric and spectrophotometric observations. In addition, we test for correlations with other combinations, including the more easily measured uniform-disk radius, but find no significant correlation in that case.

The method outlined here builds upon the technique described by Neilson & Lester (2012), but it does not employ a specific limb-darkening law with ad-hoc coefficients that can be sensitive to the quality of the observations (*e.g.* Dominik 2004). By focusing on angular diameters, one can employ more readily available observations from a plethora of sources, such as interferometry and lunar occultations, that can be coupled with spectrophotometric and/or spectroscopic observations. Our

preliminary test of the method is based on the interferometric data of Wittkowski et al. (2004). It demonstrates that spherical atmosphere models, plus the correlations derived here, provide realistic fits to the radii and masses of giant stars and presumably supergiant stars as well.

We chose here to consider stars with stellar extensions large enough that the ratio $(\theta_{\text{LD}} - \theta_{\text{Ross}})/\theta_{\text{Ross}}$ will have small uncertainties when measured by optical interferometry, but the method is not strictly limited to evolved or cool stars. To further validate it, interferometric observations will need to be carried out on stars that can be reliably modelled by stellar atmosphere codes. In particular, in the near future we plan on observing eclipsing double-line binaries for which the masses and radii of the stars are known.

We wish to thank the referee for comments that significantly improved this work. FB acknowledges funding from NSF award AST-1445935.

REFERENCES

- Baschek, B., Scholz, M., & Wehrse, R. 1991, *A&A*, 246, 374
 Bessell, M. S., Brett, J. M., Scholz, M., & Wood, P. R. 1991, *A&AS*, 89, 335
 Böhm-Vitense, E. 1958, *ZAp*, 46, 108
 Boyajian, T. S., van Belle, G., & von Braun, K. 2014, *AJ*, 147, 47
 Castelli, F. & Kurucz, R. L. 2010, *A&A*, 520, A57
 Claret, A. 2000, *A&A*, 363, 1081
 Claret, A. & Bloemen, S. 2011, *A&A*, 529, A75
 Davis, J., Tango, W. J., & Booth, A. J. 2000, *MNRAS*, 318, 387
 Dolan, M. M., Mathews, G. J., Lam, D. D., et al. 2016, *ApJ*, 819, 7
 Dominik, M. 2004, *MNRAS*, 353, 118
 Ekström, S., Georgy, C., Eggenberger, P., et al. 2012, *A&A*, 537, A146
 Gray, D. F. 2005, *The Observation and Analysis of Stellar Photospheres*
 Gray, D. F. & Pugh, T. 2012, *AJ*, 143, 92
 Gustafsson, B., Edvardsson, B., Eriksson, K., et al. 2008, *A&A*, 486, 951
 Haubois, X., Perrin, G., Lacour, S., et al. 2009, *A&A*, 508, 923
 Hauschildt, P. H., Allard, F., Ferguson, J., Baron, E., & Alexander, D. R. 1999, *ApJ*, 525, 871
 Huber, D., Bedding, T. R., Stello, D., et al. 2010, *ApJ*, 723, 1607
 Kallinger, T., Mosser, B., Hekker, S., et al. 2010, *A&A*, 522, A1
 Kippenhahn, R., Weigert, A., & Weiss, A. 2012, *Stellar Structure and Evolution*
 Kloppenborg, B. & van Belle, G. 2015, in *Astrophysics and Space Science Library*, Vol. 408, *Astrophysics and Space Science Library*, 157
 Kurucz, R. L. 1970, *Atlas: A computer program for calculating model stellar atmospheres*
 Kurucz, R. L. 2011, *Canadian Journal of Physics*, 89, 417
 Langer, N. & Kudritzki, R. P. 2014, *A&A*, 564, A52
 Lester, J. B., Dinshaw, R., & Neilson, H. R. 2013, *PASP*, 125, 335
 Lester, J. B. & Neilson, H. R. 2008, *A&A*, 491, 633
 Lobel, A. & Dupree, A. K. 2001, *ApJ*, 558, 815
 Mihalas, D. 1978, *Stellar atmospheres 2nd edition*, W. H. Freeman and Co., San Francisco
 Montargès, M., Kervella, P., Perrin, G., et al. 2014, *A&A*, 588, 130
 Neilson, H. R., Engle, S. G., Guinan, E., et al. 2012a, *ApJ*, 745, L32
 Neilson, H. R., Langer, N., Engle, S. G., Guinan, E., & Izzard, R. 2012b, *ApJ*, 760, L18
 Neilson, H. R. & Lester, J. B. 2008, *A&A*, 490, 807
 Neilson, H. R. & Lester, J. B. 2011, *A&A*, 530, A65
 Neilson, H. R. & Lester, J. B. 2012, *A&A*, 544, A117
 Neilson, H. R. & Lester, J. B. 2013a, *A&A*, 554, A98
 Neilson, H. R. & Lester, J. B. 2013b, *A&A*, 556, A86

- Neilson, H. R., Lester, J. B., & Haubois, X. 2011, in *Astronomical Society of the Pacific Conference Series*, Vol. 451, 9th Pacific Rim Conference on Stellar Astrophysics, ed. S. Qain, K. Leung, L. Zhu, & S. Kwok, 117
- Ohnaka, K., Weigelt, G., Millour, F., et al. 2011, *A&A*, 529, A163
- Paladini, C., van Belle, G. T., Aringer, B., et al. 2011, *A&A*, 533, 27
- Richichi, A., Irawati, P., Soonthornthum, B., Dhillon, V. S., & Marsh, T. R. 2014, *AJ*, 148, 100
- Stello, D., Huber, D., Bedding, T. R., et al. 2013, *ApJ*, 765, L41
- Tsuji, T. 2000, *ApJ*, 538, 801
- van Belle, G. T., Creech-Eakman, M. J., & Hart, A. 2009, *MNRAS*, 394, 1925
- Vitense, E. 1953, *ZAp*, 32, 135
- von Braun, K., Boyajian, T. S., van Belle, G. T., et al. 2014, *MNRAS*, 438, 2413
- Wittkowski, M., Aufdenberg, J. P., Driebe, T., et al. 2006a, *A&A*, 460, 855
- Wittkowski, M., Aufdenberg, J. P., & Kervella, P. 2004, *A&A*, 413, 711
- Wittkowski, M., Hummel, C. A., Aufdenberg, J. P., & Roccatagliata, V. 2006b, *A&A*, 460, 843